JOURNAL OF VIROLOGY, Feb. 2009, p. 1602–1610 Vol. 83, No. 4
0022-538X/09/$08.00+0 doi:10.1128/JVI.01590-08

ISG15 Arg151 and the ISG15-Conjugating Enzyme UbE1L Are Important for Innate Immune Control of Sindbis Virus[▽]

Nadia V. Giannakopoulos,[1] Elena Arutyunova,[2] Caroline Lai,[1,3] Deborah J. Lenschow,[1,3] Arthur L. Haas,[2]* and Herbert Whiting Virgin[1]*

Department of Pathology and Immunology, Department of Molecular Microbiology,[1] and Department of Medicine,[3] Washington University School of Medicine, St. Louis, Missouri 63110, and Department of Biochemistry and Molecular Biology, Louisiana State University Health Sciences Center School of Medicine, New Orleans, Louisiana 70112[2]

Received 25 July 2008/Accepted 2 December 2008

Interferon (IFN)-stimulated gene 15 (ISG15) is a ubiquitin-like molecule that conjugates to target proteins via a C-terminal LRLRGG motif and has antiviral function in vivo. We used structural modeling to predict human ISG15 (hISG15) residues important for interacting with its E1 enzyme, UbE1L. Kinetic analysis revealed that mutation of arginine 153 to alanine (R153A) ablated hISG15-hUbE1L binding and transthiolation of UbcH8. Mutation of other predicted UbE1L-interacting residues had minimal effects on the transfer of ISG15 from UbE1L to UbcH8. The capacity of hISG15 R153A to form protein conjugates in 293T cells was markedly diminished. Mutation of the homologous residue in mouse ISG15 (mISG15), arginine 151, to alanine (R151A) also attenuated protein ISGylation following transfection into 293T cells. We assessed the role of ISG15-UbE1L interactions in control of virus infection by constructing double subgenomic Sindbis viruses that expressed the mISG15 R151A mutant. While expression of mISG15 protected alpha/beta-IFN-receptor-deficient (IFN-αβR$^{-/-}$) mice from lethality following Sindbis virus infection, expression of mISG15 R151A conferred no survival benefit. The R151A mutation also attenuated ISG15's ability to decrease Sindbis virus replication in IFN-αβR$^{-/-}$ mice or prolong survival of ISG15$^{-/-}$ mice. The importance of UbE1L was confirmed by demonstrating that mice lacking this ISG15 E1 enzyme were highly susceptible to Sindbis virus infection. Together, these data support a role for protein conjugation in the antiviral effects of ISG15.

A critical component of the innate immune response is the antiviral state induced by type I interferons (IFNs) (19, 46, 47). In response to viral infection and the production of IFNs, cells alter their gene expression profiles to render themselves nonpermissive for viral infection and/or replication. PKR, RNase L, and Mx are well-characterized effectors in this response (40, 43). However, experiments with mice that genetically lack one or all of these antiviral molecules clearly demonstrate that there are other important molecules induced by IFN (1, 48, 57, 58). One such gene product, IFN-stimulated gene 15 (ISG15), was originally identified as a 15-kDa protein induced by IFN (2, 22) and subsequently as a 15-kDa protein that cross-reacts with antiubiquitin antibodies (13). ISG15 resembles a diubiquitin molecule, with two domains each having significant homology to ubiquitin and other ubiquitin-like molecules (33).

Analogously to ubiquitin, ISG15 is synthesized in a proform which is processed to reveal a C-terminal LRLRGG motif (41). ISG15 conjugates to target proteins via an isopeptide bond using a series of IFN-induced enzymes: an E1-activating enzyme, UbE1L (53); E2-conjugating enzyme UbcH8/UbcM8 (20, 55); E3 ligase enzymes Herc5 (4, 49, 51), HHARI (36), and Efp (59); and a deconjugating enzyme, UBP43 (28). Recent studies have confirmed that the activation of ISG15 by UbE1L is critical for protein ISGylation. Both UbE1L-deficient cells and UbE1L-deficient mice lack ISG15 conjugates following stimulation with IFN and lipopolysaccharide (21).

Recent data from both in vivo and in vitro studies demonstrated that ISG15 has antiviral function. In vivo, the expression of ISG15 from a recombinant Sindbis virus protects alpha/beta-IFN-receptor-deficient (IFN-αβR$^{-/-}$) (24), ISG15$^{-/-}$ (25), and CD1 (54) mice against lethality following Sindbis virus infection. In addition, ISG15-deficient mice display increased susceptibility to infection with Sindbis virus, herpes simplex virus type 1, gammaherpesvirus 68, and influenza A and B viruses (25). In vitro, ISG15 induction correlates with IFN-ω-mediated suppression of human immunodeficiency virus (HIV) replication, and ISG15 overexpression results in a decrease in cytoplasmic HIV transcripts and HIV protein synthesis (23) as well as decreased alphavirus replication (54). Furthermore, ISG15 and UbE1L overexpression inhibits HIV replication and interferes with the ubiquitination of Tsg101 and Gag, which are required for HIV binding and release (34). Together, these results have defined ISG15 as a critical IFN-induced antiviral molecule.

ISG15's mechanism of antiviral action is not completely defined. The existence of an IFN-inducible pathway that mirrors ubiquitin conjugation has led to the hypothesis that protein ISGylation may be an important component of the IFN-induced innate immune response (12). A role for protein conjugation in ISG15's antiviral function is suggested by the finding that heterologous expression of a conjugation-deficient form of ISG15 (LRLRAA) does not result in protection of IFN-

* Corresponding author. Mailing address for Arthur L. Haas: Department of Biochemistry and Molecular Biology, LSUHSC, 1901 Perdido Street, New Orleans, LA 70112. Phone: (504) 568-3004. Fax: (504) 568-3370. E-mail: ahaas@lsuhsc.edu. Mailing address for Herbert Whiting Virgin: Department of Pathology and Immunology, Washington University, 660 S. Euclid Ave, Box 8118, St. Louis, MO 63110. Phone: (314) 362-9223. Fax: (314) 362-4096. E-mail: virgin@wustl.edu.

▽ Published ahead of print on 10 December 2008.

$\alpha\beta R^{-/-}$ (24) or $ISG15^{-/-}$ (25) mice from lethality. Additional support for this hypothesis is that protein ISGylation is targeted by two viral immune evasion molecules. The NS1 protein of influenza B virus binds human ISG15 (hISG15) (52) and inhibits protein ISGylation (53), while an ovarian tumor domain-containing protease found in nairoviruses and arteriviruses deconjugates ISGylated proteins and abrogates ISG15's protective antiviral function (9).

Unconjugated ISG15 has also been demonstrated to have antiviral functions. In cell culture, overexpression of ISG15 can inhibit budding of Ebola virus VP40 viruslike particles (VLPs) by interacting with the Nedd4 ubiquitin ligase and inhibiting the ubiquitination of VP40 (29, 35). Additionally, ISG15 has been found in the serum of volunteers treated with IFN-β–serine (6) and mice infected with influenza virus (25), suggesting that it may also function as a cytokine. Stimulation of human peripheral blood lymphocytes with ISG15 induces NK cell proliferation, augments lymphokine-activated killer activity, and stimulates IFN-γ production (5, 42) but requires processing of pro-ISG15 to expose the two C-terminal glycine residues of ISG15's LRLRGG sequence (5). ISG15 constitutively produced by a melanoma cell line induces human dendritic cell maturation (39). Mouse ISG15 (mISG15) was reported as a neutrophil chemotactic factor during murine malarial infection with neutrophil-recruiting properties both in vitro and in vivo (38). Thus, ISG15 likely has both conjugation-dependent and conjugation-independent activities.

To further explore the role of protein ISGylation in ISG15's antiviral function, we analyzed the importance of the interaction of ISG15 with its E1 enzyme, UbE1L, in protein conjugation and in ISG15's antiviral function. By specifically targeting an interaction within the protein ISGylation pathway, we aspired to create a conjugation-deficient mutant of ISG15 which retains the C-terminal glycines in the LRLRGG sequence. We used structure-based mutagenesis to identify residues in hISG15 that are required for interaction with UbE1L and for conjugation of hISG15. Using these data, we mutagenized the homologous amino acid in mISG15 and analyzed the effect of these mutations on protein ISGylation and the antiviral effects of ISG15 in vivo. We found that mutation of hISG15 R153A mutations reduced hISG15-hUbE1L binding and disrupted protein ISGylation in 293T cells. Mutation of mISG15 R151A diminished both conjugation to target proteins and ISG15-mediated protection from Sindbis virus lethality in IFN-$\alpha\beta R^{-/-}$ and $ISG15^{-/-}$ mice. Additionally, mice lacking ISG15's E1 enzyme UbE1L had increased susceptibility to lethality following Sindbis virus infection. These data further support the conclusion that protein conjugation plays a critically important role in the antiviral effects of ISG15 in vivo by demonstrating the importance of mISG15 Arg151 and UbE1L in innate immune control of Sindbis virus infection.

MATERIALS AND METHODS

Expression of wild-type and mutant hISG15. Recombinant hISG15N13Y/C78S (hereafter referred to as hISG15), harboring an Asn13-to-Tyr mutation in the amino-terminal β-grasp domain to provide a solvent-accessible site for radioiodination and a Cys78-to-Ser mutation to stabilize the resulting protein, was expressed in *Escherichia coli* AR58 cells. Cells harboring pGEX-ISG15N13Y/C78S are an adaptation of earlier methods (33). Expression in AR58 precluded the requirement for an arginine capping residue to prevent inactivation of the recombinant glutathione *S*-transferase (GST)–hISG15 by the periplasmic carboxypeptidase noted previously (32, 33). Mutant hISG15 proteins were generated by the overlap extension PCR method using pGEX-hISG15N13Y/C78S as a template (17). The GST-hISG15 proteins were isolated by glutathione-Sepharose chromatography, processed with thrombin, and purified to apparent homogeneity by Mono Q fast protein liquid chromatography (33). Protein was quantified spectrophotometrically using an empirical 280-nm extinction coefficient of 0.885 ml/mg (33). A portion of the recombinant proteins was radioiodinated by the chloramine T procedure to yield a specific radioactivity typically in the range of 3×10^4 to 5×10^4 cpm/pmol (32, 33).

Expression of hUbE1L and UbcH8. Recombinant human GST-UbE1L (herein referred to as hUbE1L) was expressed in Sf9 cells harboring pFASTBacHsUbE1L and purified to apparent homogeneity by glutathione-Sepharose chromatography. Active hUbE1L was quantified by its stoichiometric formation of ^{125}I-ISG15 thiolester (33). Human UbcH8 was expressed by IPTG (isopropyl-β-D-thiogalactopyranoside) induction of *E. coli* BL21(DE3) harboring pGEXHsUbcH8. GST-UbcH8 was isolated by glutathione-Sepharose chromatography, processed with thrombin, and purified to apparent homogeneity by Mono Q fast protein liquid chromatography (45). Active UbcH8 was quantified by the stoichiometric formation of ^{125}I-ISG15 thiolester (14).

Transthiolation kinetic assays. The effect of additional point mutations within hISG15N13Y/C78S was quantified kinetically by monitoring the initial rates of UbcH8–^{125}I-ISG15 thiolester formation under conditions identical to those used for ^{125}I-ubiquitin transthiolation by hUba1 (45). Incubation mixtures of 25-μl final volume contained 50 mM Tris-HCl (pH 7.5), 2 mM ATP, 10 mM $MgCl_2$, 1 mM dithiothreitol, 22 nM hUbE1L, 500 nM UbcH8, and various concentrations of the ^{125}I-hISG15 mutant. Reaction mixtures were incubated for 2 min at 37°C under initial velocity conditions and quenched by the addition of 25 μl of sodium dodecyl sulfate sample buffer without β-mercaptoethanol. The UbcH8–^{125}I-hISG15 thiolester was resolved from free ^{125}I-hISG15 by sodium dodecyl sulfate-polyacrylamide gel electrophoresis. Gels were dried and autoradiographed, and UbcH8 thiolester was quantified by excising the bands from the gel and γ counting. The absolute amount of thiolester was calculated using the specific radioactivity of the ^{125}I-hISG15 (14, 45). Kinetic constants were determined by nonlinear regression analysis (45).

Eukaryotic ISG15 expression constructs. pGEX-hISG15N13Y/C78S and mutant hISG15 constructs were digested with BamHI and XhoI. Inserts were gel purified and subcloned into BamHI and XhoI sites in pcDNA4HisMaxC (Invitrogen). The N13Y and C78S mutations were reverted to wild type in pcDNA4HisMaxC-hISG15 constructs using the QuikChange Multi site-directed mutagenesis kit (Stratagene, La Jolla, CA). Nucleotides 1 to 465 of mISG15 were PCR amplified, adding a 5′ HindIII site and a 3′ KpnI site to facilitate subcloning into pCDNA3.1(+) (Invitrogen, Carlsbad, CA). Using a QuikChange kit (Stratagene), site-directed mutagenesis was performed on mISG15 nucleotides 451 to 453, CGC (Arg) to GCC (Ala), to generate mouse ISG15 mutant mISG15 R151A. All insert sequences were confirmed by sequencing.

Cell culture and transfection. 293T, BHK-21, and $ISG15^{-/-}$ murine embryonic fibroblasts (MEFs) were cultured in D10, consisting of Dulbecco modified Eagle medium (Cellgro; Mediatech, Herndon, VA) supplemented with 10% low-endotoxin fetal bovine serum (HyClone, Logan, UT), 100 U/ml penicillin, 100 μg/ml streptomycin, 10 mM HEPES, 1 mM sodium pyruvate, and 2 mM L-glutamine (Biosource, Camarillo, CA). pCAGGS.MCS and eukaryotic expression plasmids encoding hUbE1L, UbcM8, and UbcH8 were kindly provided by Dong-Er Zhang (20). Herc5 was kindly provided by Motoaki Ohtsubo (Kurume University, Fukuoka-ken, Japan). mUbE1L was PCR amplified from an IFN-β-induced bone marrow macrophage cDNA library (20) and subcloned into pCRBlunt (Invitrogen). PCR amplification with a 5′ primer containing an EcoRI site and a hemagglutinin tag and a 3′ primer containing an XhoI site generated a product that was cloned into pCAGGS.MCS. 293T cells were transfected as described previously (20) and harvested 36 h (hISG15) or 24 and 36 h (mISG15) posttransfection. Each transfection experiment was performed a minimum of three times. $ISG15^{-/-}$ MEFs were transfected using the Amaxa (Gaithersburg, MD) nucleofection system. MEFs (2×10^6) were resuspended in 100 μl buffer T and transferred to a cuvette containing either 10 μg pCAGGS-green fluorescent protein (GFP) or 1 μg pCAGGS-GFP with 9 μg mISG15 or mISG15 R151A in equal volumes. Cells were transfected using program T-20 and recovered by addition of prewarmed D10. Each transfection was plated in one well of a six-well plate, and 18 to 24 h after transfection, cells were treated with 100 U/ml IFN-β (PBL Biomedical, Piscataway, NJ) for 36 h.

Western blotting. Cells were lysed on ice in equal volumes of Laemmli sample buffer containing protease inhibitor cocktail III (Sigma). Samples were boiled for 10 min, and equal volumes were separated on a 4 to 20% gradient gel (Bio-Rad, Hercules, CA) and transferred to polyvinylidene difluoride (GE Health Sciences, Piscataway, NJ). mISG15 and mISG15 conjugates were detected using anti-

mISG15 antibodies 2D12 and 3C2 as previously described (24). Six-His-hISG15 was detected using a 1:3,000 dilution of a mouse monoclonal anti-His antibody (GE Healthcare). Rabbit polyclonal anti-Sindbis virus was a kind gift from Dianne Griffin (Johns Hopkins University, Baltimore, MD) (26) and was used at a 1:20,000 dilution. For loading controls, antivalosin-containing protein clone H-120 (Santa Cruz Biotechnology, Santa Cruz, CA) and anti-β-actin monoclonal antibody clone SC-74 (Sigma, St. Louis, MO) were used at 1:500 and 1:3,000 dilutions, respectively. Polyclonal rabbit immunoglobulin fraction anti-GFP (Molecular Probes/Invitrogen) was diluted 1:1,000. Horseradish peroxidase-conjugated secondary antibodies were diluted 1:5,000 (Jackson ImmunoResearch, West Grove, PA), and blots were developed using ECL Plus (GE Health Sciences). To quantify mISG15 conjugate levels, blots were scanned on a Storm Phosphoimager (GE Healthcare) and analyzed using ImageQuant 5.2 (GE Healthcare). Transfection efficiency was normalized by dividing mISG15 conjugate volume by GFP volume within each sample. In each experiment, the ratio of mISG15 conjugates to GFP for mISG15 LRLRGG was arbitrarily set to 10 to allow comparison across four experiments.

Generation and characterization of recombinant Sindbis viruses. Double subgenomic Sindbis virus dsTE12Q was generated from a cDNA clone by in vitro transcription and RNA transfection of BHK-21 cells as previously described (15, 24). A Sindbis virus expressing mISG15 R151A was generated by PCR amplifying pCDNA3.1 mISG15 R151A with primers that contained 5′ and 3′ BstEII restriction sites and subcloning it into dsTE12Q. Viral stocks were produced and their titers were determined on BHK-21 cells as previously described (24). Viral ISG15 expression was assessed by Western blotting. BHK-21 cells were infected at a multiplicity of infection (MOI) of 20 with dsTE12Q- or mISG15-expressing viruses. Cells were harvested 18 h postinfection and Western blotted for mISG15 or Sindbis virus proteins. Growth curves were performed at an MOI of 5 as previously described (16).

Mouse studies. IFN-αβR$^{-/-}$ mice on the 129/SV/Pas background were initially obtained from M. Aguet, Swiss Institute of Experimental Cancer Research (Epalinges, Switzerland) (7, 31). UbE1L$^{-/-}$ (21) and ISG15$^{-/-}$ mice and ISG15$^{+/+}$ littermate controls (37) have been described previously. All mice were bred and maintained at Washington University School of Medicine in accordance with all federal and university guidelines. Eight- to 10-week-old male IFN-αβR$^{-/-}$ mice were infected subcutaneously (s.c.) in the left hind footpad with 5×10^6 PFU of virus diluted in 50 μl of Hanks' balanced salt solution. Mice were followed for lethality or sacrificed on day 3, 5, or 7 to assess viral titer. Titers were by determined by plaque assay on BHK cells (24). The limit of detection of the assay is 50 PFU for all organs. Four-day-old ISG15$^{-/-}$ mice, ISG15$^{+/+}$ littermates, UbE1L$^{-/-}$ mice, or C57/BL6 pups were infected in the right cerebral hemisphere with 1,000 PFU of virus in 10 μl of Hanks' balanced salt solution and followed for lethality. To control for nutritional status and pup health, all litters contained six to eight pups with an average weight per pup of 2.1 g to 2.5 g.

Statistical analyses. All data were analyzed with Prism software (GraphPad, San Diego, CA). Growth curves were analyzed using one-way analysis of variance. Survival data were analyzed by the log-rank (Mantel-Cox) test, with death as the primary variable. Acute titer data were analyzed using the Mann-Whitney test.

RESULTS

Generation and kinetic characterization of hISG15 point mutants. To examine the interactions of ISG15 with UbE1L, we mutated ISG15 residues predicted to interact with UbE1L. Narasimhan et al. have previously used the 3.0-Å crystal structure for Nedd8 bound to its AppBp1Uba3 heterodimeric activating enzyme as a structural model for hISG15 bound to hUbE1L (33). This simulation identified six residues as putative binding "hot spots" for interaction of hISG15 with its activating E1 enzyme (Table 1). Among these residues, several positions are not conserved with ubiquitin, providing potential residues that might contribute to the specificity of UbE1L for ISG15 rather than ubiquitin (33).

In order to assess these positions as potential binding residues for hISG15 interaction with UbE1L, we expressed and purified hISG15 mutant proteins and performed functional binding assays by measuring the kinetics of UbE1L-catalyzed transfer (transthiolation) of ISG15 to UbcH8. Previous studies with the ubiquitin- and Nedd8 E1-activating enzymes (3, 45) demonstrate that the measured transthiolation K_m is equivalent to a K_d (dissociation constant) for binding between Ub/UBL and its E1 enzyme. Related end point assays with UbE1L have demonstrated that UbcH8 is an hISG15-specific conjugating enzyme that does not function in ubiquitin conjugation under physiological conditions (8, 56).

TABLE 1. Summary of kinetic constants for ISG15 point mutants

ISG15 residue	Ubiquitin paralog	K_m (μM)	k_{cat} (s^{-1})	k_{cat}/K_m (M^{-1} s^{-1})
Wild type		0.42 ± 0.05	$(2.6 \pm 0.1) \times 10^{-2}$	6.3×10^4
Arg^{87}	Lys^6	0.44 ± 0.08	$(2.3 \pm 0.1) \times 10^{-2}$	5.2×10^4
Lys^{90}	Thr^9	1.4 ± 0.1	$(6.4 \pm 0.1) \times 10^{-2}$	4.5×10^4
Arg^{92}	Lys^{11}	2.0 ± 0.1	$(4.6 \pm 0.1) \times 10^{-2}$	2.3×10^4
Trp^{123}	Arg^{42}	1.1 ± 0.1	$(6.0 \pm 0.1) \times 10^{-2}$	5.7×10^4
Glu^{132}	Glu^{51}	2.9 ± 1.4	$(0.7 \pm 0.1) \times 10^{-2}$	0.2×10^4
Arg^{153}	Arg^{72}	Not detected	Not detected	≤86

When initial rates of UbE1L-catalyzed UbcH8 transthiolation were measured at different concentrations of ^{125}I-hISG15, the data followed hyperbolic kinetics, evidenced by the linearity of double reciprocal plots. Nonlinear regression analysis was used to calculate K_m (previously shown to be equivalent to K_d) and k_{cat}, defined as $V_{max}/[UbE1L]_o$ (33). For wild-type hISG15, the K_m of 0.42 ± 0.05 μM for binding to hUbE1L compares favorably with the K_m values of 0.8 ± 0.2 μM for ubiquitin binding to hUba1 (45) and of 0.95 ± 0.18 μM for Nedd8 binding to human AppBp1Uba3 (3), indicating that the relative affinity of these ubiquitin-like proteins for their cognate activating enzymes is conserved across paralogs. Interestingly, the k_{cat} for transthiolation of $(2.6 \pm 0.1) \times 10^{-2}$ s^{-1} is >100-fold lower than the values of 4.5 s^{-1} for Uba1 and 3.5 s^{-1} for AppBp1Uba3 (3, 45). Most of the amino acid candidates identified within the carboxyl-terminal domain of hISG15 (Table 1) show modest increases in K_m when mutated to alanine, corresponding to $\Delta\Delta G_{binding}$ of ca. 1 kcal, suggesting that binding is distributed over the surface of the domain. The largest effects occur on mutation of either Glu132 or Arg153 to alanine (Table 1). Mutation of the former residue results in a sevenfold increase in K_m and a fourfold decrease in k_{cat}, leading to an overall decrease in catalytic specificity (defined as k_{cat}/K_m) of 30-fold. Mutation of Arg153 to alanine (R153A) increases the K_m significantly so that the initial rate becomes linear with respect to $[hISG15]_o$ (data not shown), preventing estimation of both K_m and k_{cat}. We estimated k_{cat}/K_m from the linear slope of v_o versus $[hISG15]_o$, the result of which revealed that the catalytic specificity is decreased >700-fold to ≤86 M^{-1} s^{-1}. Therefore, mutation of R153A effectively inactivates hISG15 with respect to UbE1L-catalyzed activation and subsequent conjugation. Significantly, Arg153 is paralogous to Arg72 of ubiquitin, a position critical in allowing cognate activating enzymes to distinguish among ubiquitin, Nedd8, and Sumo (3, 27, 50).

Mutation of UbE1L-interacting residues affects ISG15 conjugation in vivo. To assess the effect of mutating UbE1L-interacting residues on hISG15 conjugation in vivo, we utilized a 293T transfection system to coexpress hISG15, hUbE1L, UbcH8, and Herc5. Mutation of hISG15 R153A confirmed that this residue was important for conjugation of hISG15 (Fig.

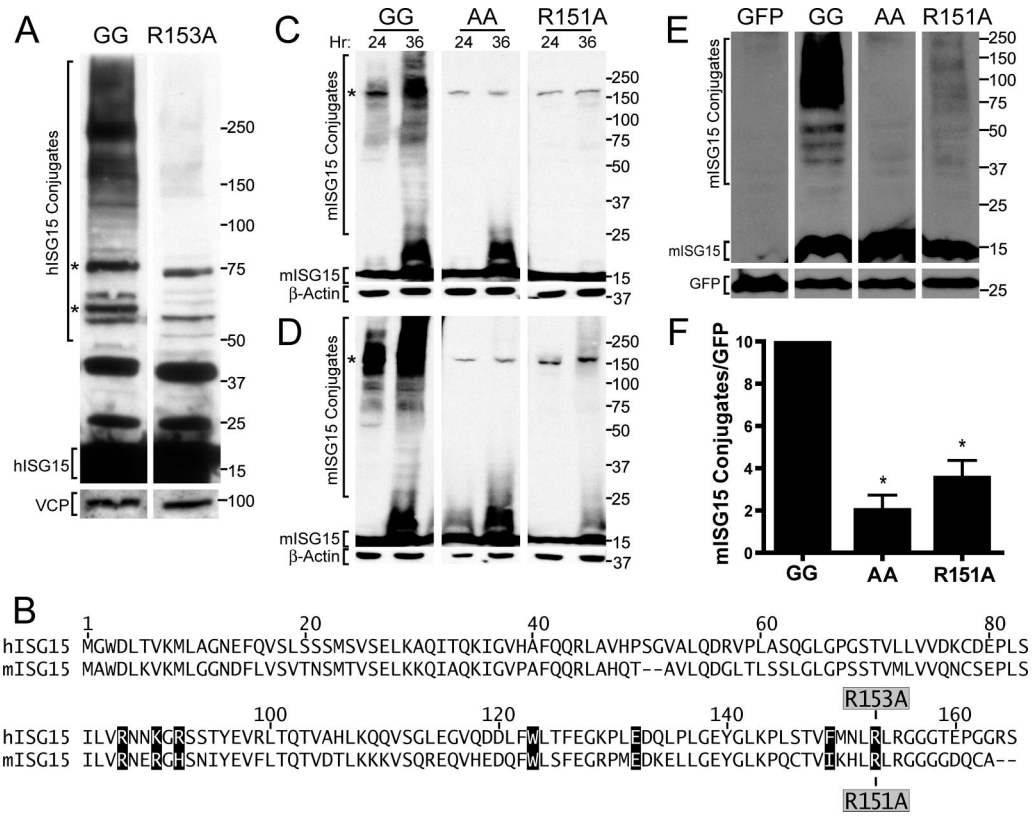

FIG. 1. Mutation of UbE1L-interacting residue arginine 153 in hISG15 affects protein conjugate formation. (A) Western blot analysis of six-His hISG15 (GG) and six-His hISG15 UbE1L-interacting mutant R153A following cotransfection with hUbE1L, UbcH8, and Herc5 into 293T cells. Asterisks indicate nonspecific bands detected in mock-transfected samples, and numbers (for panels A, C, D, and E) represent molecular mass markers (kDa). (B) Alignment of hISG15 and mISG15 sequences. Highlighted amino acids indicate ISG15 residues predicted to interact with UbE1L from hISG15 crystallization studies (33). R153A and R151A indicate hISG15 and mISG15 residues mutated in this study. (C and D) Anti-mISG15 Western blot analysis of 293T cells transfected with mISG15 LRLRGG (GG), conjugation-deficient mISG15 LRLRAA (AA), and UbE1L-interacting mutant mISG15 R151A (R151A) in the absence (C) or presence (D) of an E3 ligase, Herc5. (E) Representative anti-mISG15 Western blot analysis of IFN-β-treated ISG15$^{-/-}$ MEFs transfected with mISG15 LRLRGG (GG), mISG15 LRLRAA (AA), or mISG15 R151A (R151A) (top panel). The blot was reprobed for GFP (bottom panel). (F) Quantization of Western blot signals in panel E. Error bars represent the standard errors of the means from four experiments. One-sample *t* tests indicated that both mISG15 LRLRAA and mISG15 R151A (asterisks) were significantly different from mISG15 LRLRGG (mISG15 LRLRAA, $P = 0.0015$; 95% confidence interval, −0.264 to 4.294; mISG15 R151A, $P = 0.0045$; 95% confidence interval, 0.876 to 6.199). The graph is an arbitrary scale with mISG15 LRLRGG assigned a value of 10.

1A). As expected, wild-type hISG15 formed a characteristic ladder of protein conjugates when cotransfected with hUbE1L, UbcH8, and Herc5 (Fig. 1A). In contrast, mutation of the hUbE1L-interacting residue R153A impaired the formation of ISG15 conjugates (Fig. 1A), consistent with results observed during in vitro UbcH8 transthiolation reactions (Table 1).

Generation and conjugation of mISG15 R151A mutant. We next sought to determine the role of the UbE1L-interacting residue arginine 153 in the antiviral effects of ISG15. We have previously utilized a recombinant Sindbis virus system expressing mISG15 to demonstrate and study the antiviral activity of ISG15 (24, 25). In order to determine the importance of the ISG15/UbE1L interaction for the antiviral activity of ISG15 in vitro and in a mouse infection model, we chose to generate a mutant mISG15 construct homologous to the hISG15 R153A mutation. Alignment of hISG15 and mISG15 sequences suggested that mISG15 arginine 151 was analogous to hISG15 arginine 153, a critical UbE1L-interacting residue in hISG15 (Fig. 1B). Modeling the mISG15 structure by threading its sequence onto the hISG15 crystal structure confirmed that mISG15 Arg151 was structurally analogous to hISG15 Arg153 (data not shown). The mISG15 R151A mutant was stably expressed, as both polyclonal and monoclonal anti-mISG15 antibodies were able to detect mISG15 R151A (Fig. 1C and data not shown).

We tested the biological effect of those mutations on ISGylation of target proteins by cotransfecting constructs with mUbE1L and UbcM8. Wild-type mISG15 conjugated to cellular proteins, while a mutant form of ISG15 where the C-terminal glycines residues have been replaced with alanines (mISG15 LRLRAA) failed to form higher-molecular-weight conjugates as previously reported (24) (Fig. 1C). UbE1L-interacting mutant mISG15 R151A was impaired in its ability to form conjugates, with no conjugates being detected following mISG15 R151A expression (Fig. 1C).

To examine the effect of an E3 ligase on mISG15 mutant conjugation, we cotransfected mISG15 constructs, mUbE1L and UbcM8, with human Herc5. A mouse homologue of Herc5 has not been identified (10, 18), and Efp, the only other identified ISG15 E3 ligase, targets specific substrates and does not

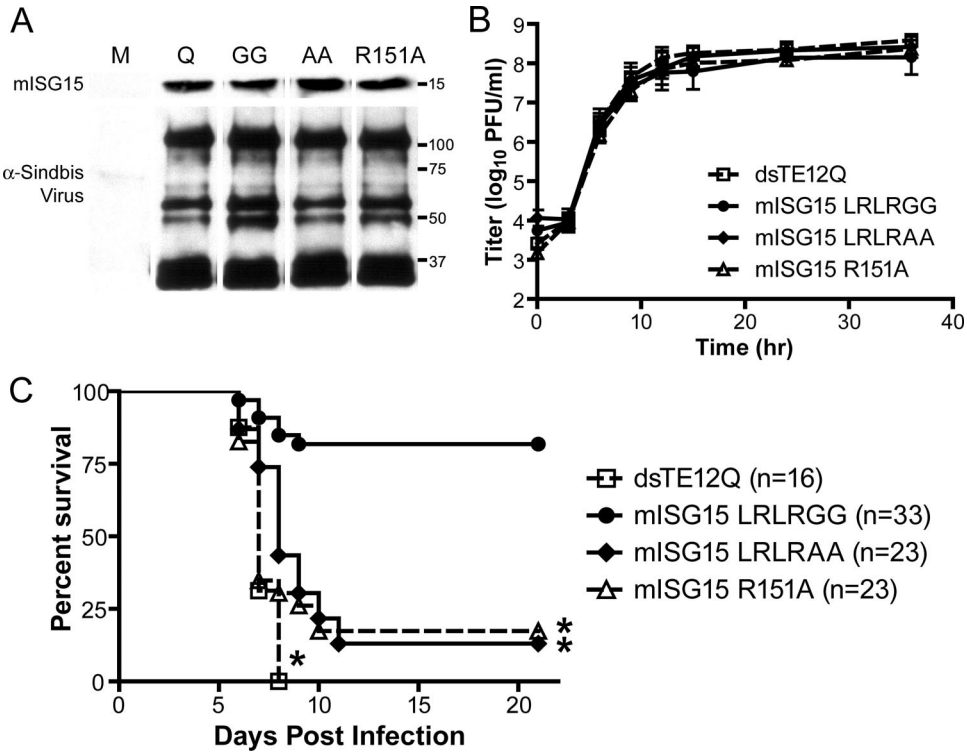

FIG. 2. Mutation of UbE1L-interacting residue Arg151 attenuates mISG15's antiviral function during Sindbis virus infection. (A) Western blot analysis of BHK-21 cells mock infected (M) or infected with parental dsTE12Q (Q) or dsTE12Q containing mISG15 LRLRGG (GG), mISG15 LRLRAA (AA), or mISG15 R151A (R151A) at an MOI of 20. Parallel blots were probed with anti-ISG15 (top panel) or polyclonal anti-Sindbis virus (bottom panel). (B) Single-step growth curves of parental (dsTE12Q) or recombinant (mISG15 LRLRGG, mISG15 LRLRAA, or mISG15 R151A) Sindbis viruses in BHK-21 cells (MOI, 5). Data are represented as means ± standard errors of the means for three (dsTE12Q) or six (recombinant viruses) replicates. There are no significant differences between the medians of different viruses when analyzed by analysis of variance ($P = 0.9993$). (C) Survival of IFN-$\alpha\beta R^{-/-}$ mice infected with 5×10^6 PFU of Sindbis viruses s.c. as indicated. The number of mice infected per group is indicated in parentheses, and data are compiled from a minimum of three experiments. Asterisks indicate curves statistically different from mISG15 LRLRGG (LRLRGG versus R151A, LRLRGG versus LRLRAA, and LRLRGG versus dsTE12Q, all $P < 0.001$).

increase global ISGylation (59). Addition of human Herc5 increased the conjugation of wild-type mISG15 to cellular targets (Fig. 1D). mISG15 LRLRAA remained unable to form conjugates, but surprisingly, a low level of mISG15 R151A conjugates were detected 36 h posttransfection (Fig. 1D). Ubiquitin conjugation utilizes several conjugating enzymes and numerous ligating enzymes. While only one E2 and three E3 ISGylation enzymes have been identified, it possible that there are additional conjugating and ligating enzymes for ISG15. If these enzymes are also IFN induced, they may not be expressed during 293T cell transfection. To provide optimal conjugation conditions with a full complement of enzymes expressed at endogenous levels, we therefore transfected ISG15$^{-/-}$ MEFs with mISG15, mISG15 LRLRAA, or mISG15 R151A and treated transfected cells with IFN-β. Similar to results obtained following 293T transfection, mutation of UbE1L-interacting residues impaired protein ISGylation in ISG15$^{-/-}$ MEFs (Fig. 1E). Both mISG15 LRLRAA and mISG15 R151A were severely compromised in their ability to form protein conjugates (Fig. 1E). As IFN-β-treated ISG15$^{-/-}$ MEFs should express all mouse IFN-induced conjugation enzymes, these data confirmed that both mISG15 LRLRAA and mISG15 R151A are severely compromised in their ability to conjugate to cellular proteins.

The mUbE1L-mISG15 interaction is important for mISG15's antiviral function. To assess the antiviral capability of mISG15 mutants, we constructed Sindbis viruses expressing mISG15, mISG15 LRLRAA, or mISG15 R151A (15). The mISG15-containing viruses expressed similar levels of mISG15 or mISG15 mutant proteins (Fig. 2A, top panel). All viruses expressed similar levels of Sindbis virus proteins (Fig. 2A, bottom panel) and grew with equivalent kinetics to comparable final titers in BHK cells (Fig. 2B).

Infection of IFN-$\alpha\beta R^{-/-}$ mice with dsTE12Q, a double-subgenomic strain of Sindbis virus, resulted in 100% lethality by day 7 postinfection (Fig. 2C). As previously demonstrated (24), expression of mISG15 LRLRGG protected mice from lethality (80% survival), while expression of mISG15 LR LRAA failed to protect IFN-$\alpha\beta R^{-/-}$ mice from lethality (13% survival) (Fig. 2C). Infection of mice with a Sindbis virus expressing mISG15 R151A resulted in a loss of protection from lethality, with only 17% of the mice surviving infection. The increase in lethality was consistent with the dramatic decrease in ISG15 conjugate formation (Fig. 1C to F) by the mISG15 R151A mutant. Additionally, the increased lethality was similar to the increase in lethality observed following infection with a virus expressing mISG15 LRLRAA, which lacks the C-ter-

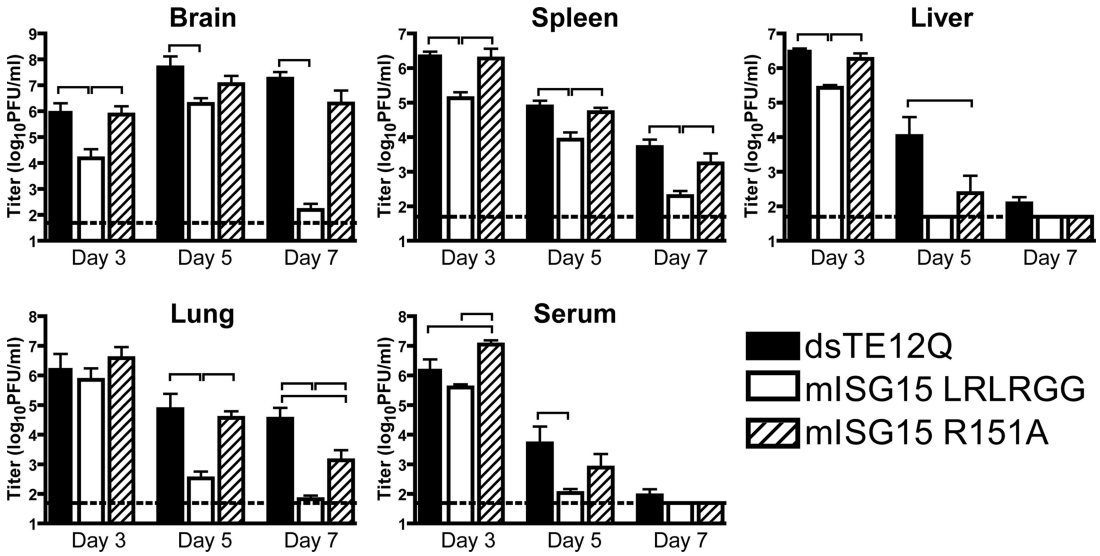

FIG. 3. ISG15 UbE1L-interacting mutant R151A is attenuated in its ability to decrease Sindbis virus replication. Viral titers of dsTE12Q, mISG15 LRLRGG, or mISG15 R151A in brains, spleen, liver, lung, and serum of IFN-αβR$^{-/-}$ mice infected for 3, 5, or 7 days. Data are pooled from two independent experiments with six mice per group. Error bars represent standard errors of the means, and the dashed line indicates the plaque assay limit of detection. Brackets denote statistically significant ($P < 0.05$) differences between indicated viruses.

minal glycines required for ISG15 conjugation to cellular proteins (24).

The replication of dsTE12Q, a neurovirulent strain of Sindbis virus, is restricted to the brain and spinal cord in wild-type mice but is disseminated in mice lacking the type I IFN receptor (24). Previous work has shown that while expression of mISG15 LRLRGG attenuated viral replication following infection, it alone did not restrict the dissemination of the virus (25). To further evaluate the effect of the mISG15 R151A mutation on the antiviral activity of ISG15, we compared organ titers following infection with recombinant Sindbis viruses expressing mISG15 LRLRGG or mISG15 R151A. Viral spread was not restricted by mISG15 R151A, as viral titers were detected in multiple organs (Fig. 3). Mutation of mISG15 R151A resulted in increased viral titers in brain, liver, spleen, and lungs (Fig. 3) of IFN-αβR$^{-/-}$ mice compared to the replication of a Sindbis virus containing mISG15 LRLRGG. These data show that mISG15 Arg151 strongly contributed to ISG15's antiviral function in IFN-αβR$^{-/-}$ mice.

Mutation of mISG15 Arg151 attenuates the antiviral function of ISG15 in Sindbis virus-infected ISG15$^{-/-}$ mice. To assess the ability of mISG15 R151A to rescue mice from lethality in the presence of an intact IFN response, ISG15$^{-/-}$ mice were infected with Sindbis viruses expressing mISG15 LRLRGG, mISG15 LRLRAA, or mISG15 R151A. As previously published, ISG15$^{-/-}$ pups display increased sensitivity to infection with dsTE12Q (25). Heterologous expression of mISG15 LRLRGG, but not mISG15 LRLRAA, significantly increased the survival among infected ISG15$^{-/-}$ pups (25) (Fig. 4). Expression of mISG15 R151A results in a statistically significant attenuation of ISG15's antiviral effect (Fig. 4), confirming that mISG15 Arg151 is important for ISG15's innate immune control of Sindbis virus infection. Interestingly, the survival curve of ISG15$^{-/-}$ mice infected with viruses expressing mISG15 R151A is also statistically different from the survival curve of mice infected with viruses expressing mISG15 LRLRAA (Fig. 4). These data indicated that mISG15 arginine 151 is critical for the antiviral effect of ISG15, but in the presence of an IFN response, this residue does not account for all of ISG15's antiviral activity.

UbE1L$^{-/-}$ mice display increased lethality following Sindbis virus infection. To further address the importance of the ISG15 E1 enzyme UbE1L in resistance to viral infection,

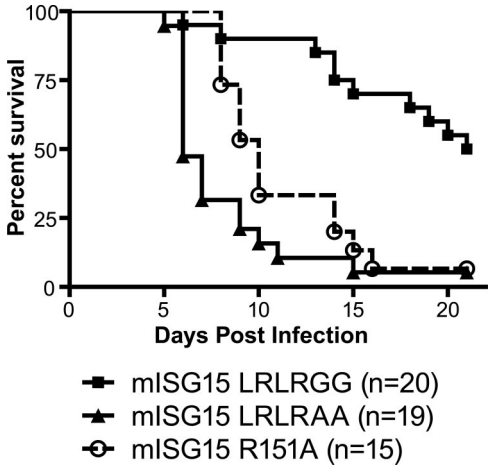

FIG. 4. mISG15 UbE1L-interacting mutants prolong survival during Sindbis virus infection. Survival of ISG15$^{-/-}$ pups infected with 1,000 PFU intracerebrally of virus expressing either mISG15 LRL RGG, mISG15 LRLRAA, or mISG15 R151A. Data are pooled from two (mISG15 R151A) or three (mISG15 LRLRGG and mISG15 LR LRAA) experiments, and the numbers of mice per group are indicated in parentheses. *P* values for comparisons between survival curves are as follows: mISG15 R151A versus mISG15 LRLRGG, $P = 0.0002$; mISG15 R151A versus mISG15 LRLRAA, $P = 0.0365$; mISG15 LR LRGG versus mISG15 LRLRAA, $P < 0.0001$.

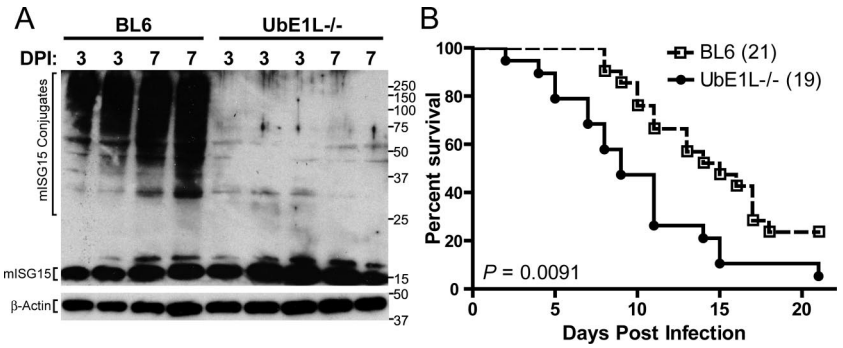

FIG. 5. UbE1L$^{-/-}$ mice display increased susceptibility to Sindbis virus infection. (A) Anti-mISG15 Western blot analysis of brains from BL6 or UbE1L$^{-/-}$ mice infected with 5×10^6 PFU of dsTE12Q s.c. on day 3 or 7 postinfection. Parallel blots were probed with anti-mISG15 (top panel) or anti-β-actin (bottom panel). DPI, day postinfection. (B) Survival of UbE1L$^{-/-}$ and BL6 mice following infection with 5×10^6 PFU of dsTE12Q s.c. *P* values of log-rank comparisons between UbE1L$^{-/-}$ and BL6 mouse survival curves are shown.

UbE1L-deficient mice (21) were infected with Sindbis virus strain dsTE12Q. Previous work has shown that cells isolated from UbE1L$^{-/-}$ mice express free ISG15 but are unable to form ISG15 conjugates (21). Similarly, brain tissue from UbE1L$^{-/-}$ mice contains no detectable ISG15 conjugates 3 or 7 days post-dsTE12Q infection, while wild-type BL6 mice had ISG15 conjugates at both time points (Fig. 5A). Following infection with dsTE12Q, UbE1L$^{-/-}$ mice display increased lethality compared to BL6 wild-type mice (Fig. 5B). The increased lethality noted in UbE1L$^{-/-}$ mice is similar to the reported increased susceptibility of ISG15$^{-/-}$ mice to dsTE12Q infection (25) and shows that UbE1L is important for innate control of Sindbis virus infection.

DISCUSSION

To investigate the importance of the ISG15-UbE1L binding in ISG15's antiviral function, we performed alanine mutagenesis on ISG15 amino acids predicted to interact with UbE1L. In vitro kinetic analysis of hISG15 mutants suggested that arginine 153 was a critical residue in the UbE1L-ISG15 interaction, while mutation of other predicted UbE1L-interacting residues in ISG15 had a more modest effect on binding (Table 1). In cultured cells, mutation of hISG15 R153A greatly decreased protein ISGylation in a 293T cell conjugation system (Fig. 1A), confirming the importance of ISG15-UbE1L binding for protein ISGylation.

To confirm that mutation of residues important for ISG15-UbE1L binding would disrupt ISG15's antiviral activity, we utilized a recombinant Sindbis virus system to express ISG15 in mice deficient in type I IFN signaling or ISG15 itself (24, 25). As hISG15 has not been tested in this mouse system, we mutated the mISG15 residue analogous to hISG15 Arg153 (Fig. 1B), allowing us to translate our kinetic analysis of the ISG15-UbE1L interaction into an in vivo antiviral function. Mutation of either hISG15 R153A or mISG15 R151A resulted in a significant diminution of protein ISGylation following transfection into 293T cells (Fig. 1). Additionally, transfection of mISG15 R151A into IFN-β-stimulated ISG15$^{-/-}$ MEFs resulted in minimal protein ISGylation (Fig. 1E and F). As all IFN-β-induced conjugation enzymes should be expressed under these conditions, these data confirm that mutation of mISG15 151A significantly impacts protein ISGylation even under potentially optimal conjugation conditions.

As expected from prior studies, mISG15 LRLRGG forms abundant conjugates in a 293T transfection system, protects IFN-αβR$^{-/-}$ and ISG15$^{-/-}$ mice from lethality, and results in decreased viral titers in infected IFN-αβR$^{-/-}$ mice (24). Mutation of the terminal two glycines of mISG15 (mISG15 LRL RAA) abolishes protein conjugation and eliminates the capacity of ISG15 to protect from lethality during infection of IFN-αβR$^{-/-}$ and ISG15$^{-/-}$ mice (Fig. 1 and 2) (24, 25). It has previously been shown that Sindbis viruses expressing mISG15 LRLRAA grow to higher titers than do viruses expressing mISG15 in IFN-αβR$^{-/-}$ mice (24).

Infection of IFN-αβR$^{-/-}$ mice with Sindbis viruses expressing the mISG15 R151A mutation resulted in increased lethality and viral titer (Fig. 2 and 3). Additionally, mutation of mISG15 R151A resulted in increased lethality following infection of ISG15$^{-/-}$ mice (Fig. 4), confirming that this residue is important for ISG15-mediated control of Sindbis virus infection. Data from our kinetic analysis (Table 1) demonstrated that hISG15 Arg153, the residue analogous to mISG15 Arg151, is critical for ISG15-UbE1L binding and that mutation of either hISG15 Arg153 or mISG15 Arg151 drastically impairs protein ISGylation (Fig. 1). As such, we hypothesize that by mutating mISG15 Arg151, we are disrupting the ISG15-UbE1L interaction and interfering with the ISG15-mediated control of Sindbis virus infection. As the last four amino acids (LRGG) of ISG15 are disordered and not visualized in the ISG15 crystal structure (33), it is unlikely that mutation of hISG15 R151/mISG15 R153 is inhibiting conjugation by altering the structure of the diglycine moiety. Additionally, we demonstrate that UbE1L is important for control of Sindbis virus infection, as mice deficient in UbE1L and protein ISGylation display increased sensitivity to Sindbis virus infection (Fig. 5). These data are consistent with the hypothesis that ISG15-UbE1L binding, mISG15 Arg151, and protein ISGylation are important components of ISG15's antiviral function.

ISG15 has been proposed to have both conjugation-dependent and conjugation-independent antiviral functions. Interestingly, infection of ISG15$^{-/-}$ mice with recombinant Sindbis viruses expressing mISG15 R151A resulted in a small, but statistically significant, increase in survival compared to that

with expression of mISG15 LRLRAA (Fig. 4), while infection of mice lacking type I IFN signaling showed no difference in survival from that of mice with type I IFN signaling (Fig. 2). This suggests that, in a system which lacks only ISG15 but retains other IFN-induced genes, mISG15 R151A contributes an antiviral activity not found in mISG15 LRLRAA.

In vivo conjugation in 293T cells and ISG15$^{-/-}$ MEFs demonstrates that mISG15 R151A retains a small amount of residual conjugating activity (Fig. 1D and F). One significant difference between ISG15$^{-/-}$ and IFN-αβR$^{-/-}$ mice is the presence or absence of additional IFN-stimulated genes, including ISG15's E1, E2, and E3 enzymes. ISG15 mRNA expression can be induced in an IFN-αβ-independent manner (11, 30, 44). In contrast, ISG15$^{-/-}$ mice should express all of the ISG15 conjugating machinery at levels approximating those in wild-type animals; in the presence of higher levels of conjugating enzymes in ISG15$^{-/-}$ mice, any residual conjugating ability of mISG15 R151A could be amplified and result in increased survival. The increase in survival seen in ISG15$^{-/-}$ mice suggests that the small number of residual conjugates formed by mISG15 R151A (Fig. 1) could have significant physiologic importance.

Alternatively, the difference in lethality could reflect additional, non-conjugation-dependent functions of mISG15 found in mISG15 R151A but not mISG15 LRLRAA. Recent data have demonstrated that intracellular expression of free ISG15 can inhibit budding of Ebola virus VP40 VLPs by interacting with the Nedd4 ubiquitin ligase and inhibiting the ubiquitination of VP40 (29, 35). While expression of ISG15's conjugating enzymes was not required for the antiviral activity of ISG15 in these systems, the molecular determinants of ISG15 required were not determined. Additionally, it has previously been reported that the extracellular cytokine function of hISG15 requires exposure of the terminal two glycine residues (5). In our constructs, the terminal two diglycine residues are mutated in mISG15 LRLRAA but not mISG15 R151A (LALRGG).

We have demonstrated that mISG15 Arg151 is critical for protein conjugation and that mISG15 Arg151 and UbE1L play an important role in the control of Sindbis virus infection by ISG15. In the face of overwhelming immunocompromise in IFN-αβR$^{-/-}$ mice, protein ISGylation contributes the majority of ISG15's antiviral effect, with the contribution of a small amount of conjugates or an additional, conjugation-independent antiviral activity being minimal. These data confirm previous observations that conjugation-deficient forms of ISG15 are impaired in their antiviral activity and demonstrate that mISG15 Arg151 is a critical residue in ISG15's antiviral function.

ACKNOWLEDGMENTS

This work was funded by grants GM34007 and GM47426 (A.L.H.) and by NIAID grant U54 AI057160 projects 6 and 10 (H.W.V.).

We thank Darren Kraelemeyer and Lindsay Droit for technical assistance.

REFERENCES

1. **Abraham, N., D. F. Stojdl, P. I. Duncan, N. Methot, T. Ishii, M. Dube, B. C. Vanderhyden, H. L. Atkins, D. A. Gray, M. W. McBurney, A. E. Koromilas, E. G. Brown, N. Sonenberg, and J. C. Bell.** 1999. Characterization of transgenic mice with targeted disruption of the catalytic domain of the double-stranded RNA-dependent protein kinase, PKR. J. Biol. Chem. **274:**5953–5962.
2. **Blomstrom, D. C., D. Fahey, R. Kutny, B. D. Korant, and E. Knight, Jr.** 1986. Molecular characterization of the interferon-induced 15-kDa protein. Molecular cloning and nucleotide and amino acid sequence. J. Biol. Chem. **261:**8811–8816.
3. **Bohnsack, R. N., and A. L. Haas.** 2003. Conservation in the mechanism of Nedd8 activation by the human AppBp1-Uba3 heterodimer. J. Biol. Chem. **278:**26823–26830.
4. **Dastur, A., S. Beaudenon, M. Kelley, R. M. Krug, and J. M. Huibregtse.** 2006. Herc5, an interferon-induced HECT E3 enzyme, is required for conjugation of ISG15 in human cells. J. Biol. Chem. **281:**4334–4338.
5. **D'Cunha, J., E. Knight, Jr., A. L. Haas, R. L. Truitt, and E. C. Borden.** 1996. Immunoregulatory properties of ISG15, an interferon-induced cytokine. Proc. Natl. Acad. Sci. USA **93:**211–215.
6. **D'Cunha, J., S. Ramanujam, R. J. Wagner, P. L. Witt, E. Knight, Jr., and E. C. Borden.** 1996. In vitro and in vivo secretion of human ISG15, an IFN-induced immunomodulatory cytokine. J. Immunol. **157:**4100–4108.
7. **Dunn, G. P., A. T. Bruce, K. C. Sheehan, V. Shankaran, R. Uppaluri, J. D. Bui, M. S. Diamond, C. M. Koebel, C. Arthur, J. M. White, and R. D. Schreiber.** 2005. A critical function for type I interferons in cancer immunoediting. Nat. Immunol. **6:**722–729.
8. **Durfee, L. A., M. L. Kelley, and J. M. Huibregtse.** 2008. The basis for selective E1-E2 interactions in the ISG15 conjugation system. J. Biol. Chem. **283:**23895–23902.
9. **Frias-Staheli, N., N. V. Giannakopoulos, M. Kikkert, S. L. Taylor, A. Bridgen, J. J. Paragas, J. A. Richt, R. R. Rowland, C. S. Schmaljohn, D. J. Lenschow, E. J. Snijder, A. Garcia-Sastre, and H. W. Virgin IV.** 2007. Ovarian tumor domain-containing viral proteases evade ubiquitin- and ISG15-dependent innate immune responses. Cell Host Microbe **2:**404–416.
10. **Garcia-Gonzalo, F. R., and J. L. Rosa.** 2005. The HERC proteins: functional and evolutionary insights. Cell. Mol. Life Sci. **62:**1826–1838.
11. **Geiss, G., G. Jin, J. Guo, R. Bumgarner, M. G. Katze, and G. C. Sen.** 2001. A comprehensive view of regulation of gene expression by double-stranded RNA-mediated cell signaling. J. Biol. Chem. **276:**30178–30182.
12. **Haas, A. L.** 2006. ISG15-dependent regulation, p. 103–131. *In* R. J. Mayer, A. Ciechanover, and M. Rechsteiner (ed.), Protein degradation: cell biology of the ubiquitin-proteasome system. Wiley Interscience, New York, NY.
13. **Haas, A. L., P. Ahrens, P. M. Bright, and H. Ankel.** 1987. Interferon induces a 15-kilodalton protein exhibiting marked homology to ubiquitin. J. Biol. Chem. **262:**11315–11323.
14. **Haas, A. L., and P. M. Bright.** 1988. The resolution and characterization of putative ubiquitin carrier protein isozymes from rabbit reticulocytes. J. Biol. Chem. **263:**13258–13267.
15. **Hardwick, J. M., and B. Levine.** 2000. Sindbis virus vector system for functional analysis of apoptosis regulators. Methods Enzymol. **322:**492–508.
16. **Heise, M. T., D. A. Simpson, and R. E. Johnston.** 2000. A single amino acid change in nsP1 attenuates neurovirulence of the Sindbis-group alphavirus S.A.AR86. J. Virol. **74:**4207–4213.
17. **Ho, S. N., H. D. Hunt, R. M. Horton, J. K. Pullen, and L. R. Pease.** 1989. Site-directed mutagenesis by overlap extension using the polymerase chain reaction. Gene **77:**51–59.
18. **Hochrainer, K., H. Mayer, U. Baranyi, B. Binder, J. Lipp, and R. Kroismayr.** 2005. The human HERC family of ubiquitin ligases: novel members, genomic organization, expression profiling, and evolutionary aspects. Genomics **85:**153–164.
19. **Isaacs, A., and J. Lindenmann.** 1957. Virus interference. 1. The interferon. Proc. R. Soc. Lond. B Biol. Sci. **147:**258–267.
20. **Kim, K. I., N. V. Giannakopoulos, H. W. Virgin, and D. E. Zhang.** 2004. Interferon-inducible ubiquitin E2, Ubc8, is a conjugating enzyme for protein ISGylation. Mol. Cell. Biol. **24:**9592–9600.
21. **Kim, K. I., M. Yan, O. Malakhova, J. K. Luo, M. F. Shen, W. Zou, J. C. de la Torre, and D. E. Zhang.** 2006. Ube1L and protein ISGylation are not essential for alpha/beta interferon signaling. Mol. Cell. Biol. **26:**472–479.
22. **Korant, B. D., D. C. Blomstrom, G. J. Jonak, and E. Knight, Jr.** 1984. Interferon-induced proteins. Purification and characterization of a 15,000-dalton protein from human and bovine cells induced by interferon. J. Biol. Chem. **259:**14835–14839.
23. **Kunzi, M. S., and P. M. Pitha.** 1996. Role of interferon-stimulated gene ISG-15 in the interferon-omega-mediated inhibition of human immunodeficiency virus replication. J. Interferon Cytokine Res. **16:**919–927.
24. **Lenschow, D. J., N. V. Giannakopoulos, L. J. Gunn, C. Johnston, A. K. O'Guin, R. E. Schmidt, B. Levine, and H. W. Virgin.** 2005. Identification of interferon-stimulated gene 15 as an antiviral molecule during Sindbis virus infection in vivo. J. Virol. **79:**13974–13983.
25. **Lenschow, D. J., C. Lai, N. Frias-Staheli, N. V. Giannakopoulos, A. Lutz, T. Wolff, A. Osiak, B. Levine, R. E. Schmidt, A. Garcia-Sastre, D. A. Leib, A. Pekosz, K. P. Knobeloch, I. Horak, and H. W. Virgin.** 2007. IFN-stimulated gene 15 functions as a critical antiviral molecule against influenza, herpes, and Sindbis viruses. Proc. Natl. Acad. Sci. USA **104:**1371–1376.
26. **Levine, B., J. E. Goldman, H. H. Jiang, D. E. Griffin, and J. M. Hardwick.** 1996. Bc1-2 protects mice against fatal alphavirus encephalitis. Proc. Natl. Acad. Sci. USA **93:**4810–4815.
27. **Lois, L. M., and C. D. Lima.** 2005. Structures of the SUMO E1 provide

mechanistic insights into SUMO activation and E2 recruitment to E1. EMBO J. **24:**439–451.
28. **Malakhov, M. P., O. A. Malakhova, K. I. Kim, K. J. Ritchie, and D. E. Zhang.** 2002. UBP43 (USP18) specifically removes ISG15 from conjugated proteins. J. Biol. Chem. **277:**9976–9981.
29. **Malakhova, O. A., and D. E. Zhang.** 2008. ISG15 inhibits Nedd4 ubiquitin E3 activity and enhances the innate antiviral response. J. Biol. Chem. **283:**8783–8787.
30. **Mossman, K. L., P. F. Macgregor, J. J. Rozmus, A. B. Goryachev, A. M. Edwards, and J. R. Smiley.** 2001. Herpes simplex virus triggers and then disarms a host antiviral response. J. Virol. **75:**750–758.
31. **Muller, U., S. Steinhoff, L. F. L. Reis, S. Hemmi, J. Pavlovic, R. M. Zinkernagel, and M. Aguet.** 1994. Functional role of type I and type II interferons in antiviral defense. Science **264:**1918–1921.
32. **Narasimhan, J., J. L. Potter, and A. L. Haas.** 1996. Conjugation of the 15-kDa interferon-induced ubiquitin homolog is distinct from that of ubiquitin. J. Biol. Chem. **271:**324–330.
33. **Narasimhan, J., M. Wang, Z. Fu, J. M. Klein, A. L. Haas, and J. J. Kim.** 2005. Crystal structure of the interferon-induced ubiquitin-like protein ISG15. J. Biol. Chem. **280:**27356–27365.
34. **Okumura, A., G. Lu, I. Pitha-Rowe, and P. M. Pitha.** 2006. Innate antiviral response targets HIV-1 release by the induction of ubiquitin-like protein ISG15. Proc. Natl. Acad. Sci. USA **103:**1440–1445.
35. **Okumura, A., P. M. Pitha, and R. N. Harty.** 2008. ISG15 inhibits Ebola VP40 VLP budding in an L-domain-dependent manner by blocking Nedd4 ligase activity. Proc. Natl. Acad. Sci. USA **105:**3974–3979.
36. **Okumura, F., W. Zou, and D. E. Zhang.** 2007. ISG15 modification of the eIF4E cognate 4EHP enhances cap structure-binding activity of 4EHP. Genes Dev. **21:**255–260.
37. **Osiak, A., O. Utermohlen, S. Niendorf, I. Horak, and K. P. Knobeloch.** 2005. ISG15, an interferon-stimulated ubiquitin-like protein, is not essential for STAT1 signaling and responses against vesicular stomatitis and lymphocytic choriomeningitis virus. Mol. Cell. Biol. **25:**6338–6345.
38. **Owhashi, M., Y. Taoka, K. Ishii, S. Nakazawa, H. Uemura, and H. Hambara.** 2003. Identification of a ubiquitin family protein as a novel neutrophil chemotactic factor. Biochem. Biophys. Res. Commun. **309:**533–539.
39. **Padovan, E., L. Terracciano, U. Certa, B. Jacobs, A. Reschner, M. Bolli, G. C. Spagnoli, E. C. Borden, and M. Heberer.** 2002. Interferon stimulated gene 15 constitutively produced by melanoma cells induces e-cadherin expression on human dendritic cells. Cancer Res. **62:**3453–3458.
40. **Paun, A., and P. M. Pitha.** 2007. The innate antiviral response: new insights into a continuing story. Adv. Virus Res. **69:**1–66.
41. **Potter, J. L., J. Narasimhan, L. Mende-Mueller, and A. L. Haas.** 1999. Precursor processing of pro-ISG15/UCRP, an interferon-beta-induced ubiquitin-like protein. J. Biol. Chem. **274:**25061–25068.
42. **Recht, M., E. C. Borden, and E. Knight, Jr.** 1991. A human 15-kDa IFN-induced protein induces the secretion of IFN-gamma. J. Immunol. **147:**2617–2623.
43. **Sen, G. C.** 2001. Viruses and interferons. Annu. Rev. Microbiol. **55:**255–281.
44. **Sen, G. C., and S. N. Sarkar.** 2007. The interferon-stimulated genes: targets of direct signaling by interferons, double-stranded RNA, and viruses. Curr. Top. Microbiol. Immunol. **316:**233–250.
45. **Siepmann, T. J., R. N. Bohnsack, Z. Tokgoz, O. V. Baboshina, and A. L. Haas.** 2003. Protein interactions within the N-end rule ubiquitin ligation pathway. J. Biol. Chem. **278:**9448–9457.
46. **Stark, G. R., I. M. Kerr, B. R. Williams, R. H. Silverman, and R. D. Schreiber.** 1998. How cells respond to interferons. Annu. Rev. Biochem. **67:**227–264.
47. **Stetson, D. B., and R. Medzhitov.** 2006. Type I interferons in host defense. Immunity **25:**373–381.
48. **Stojdl, D. F., N. Abraham, S. Knowles, R. Marius, A. Brasey, B. D. Lichty, E. G. Brown, N. Sonenberg, and J. C. Bell.** 2000. The murine double-stranded RNA-dependent protein kinase PKR is required for resistance to vesicular stomatitis virus. J. Virol. **74:**9580–9585.
49. **Takeuchi, T., S. Inoue, and H. Yokosawa.** 2006. Identification and Herc5-mediated ISGylation of novel target proteins. Biochem. Biophys. Res. Commun. **348:**473–477.
50. **Whitby, F. G., G. Xia, C. M. Pickart, and C. P. Hill.** 1998. Crystal structure of the human ubiquitin-like protein NEDD8 and interactions with ubiquitin pathway enzymes. J. Biol. Chem. **273:**34983–34991.
51. **Wong, J. J., Y. F. Pung, N. S. Sze, and K. C. Chin.** 2006. HERC5 is an IFN-induced HECT-type E3 protein ligase that mediates type I IFN-induced ISGylation of protein targets. Proc. Natl. Acad. Sci. USA **103:**10735–10740.
52. **Yuan, W., J. M. Aramini, G. T. Montelione, and R. M. Krug.** 2002. Structural basis for ubiquitin-like ISG 15 protein binding to the NS1 protein of influenza B virus: a protein-protein interaction function that is not shared by the corresponding N-terminal domain of the NS1 protein of influenza A virus. Virology **304:**291–301.
53. **Yuan, W., and R. M. Krug.** 2001. Influenza B virus NS1 protein inhibits conjugation of the interferon (IFN)-induced ubiquitin-like ISG15 protein. EMBO J. **20:**362–371.
54. **Zhang, Y., C. W. Burke, K. D. Ryman, and W. B. Klimstra.** 2007. Identification and characterization of interferon-induced proteins that inhibit alphavirus replication. J. Virol. **81:**11246–11255.
55. **Zhao, C., S. L. Beaudenon, M. L. Kelley, M. B. Waddell, W. Yuan, B. A. Schulman, J. M. Huibregtse, and R. M. Krug.** 2004. The UbcH8 ubiquitin E2 enzyme is also the E2 enzyme for ISG15, an IFN-alpha/beta-induced ubiquitin-like protein. Proc. Natl. Acad. Sci. USA **101:**7578–7582.
56. **Zhao, C., C. Denison, J. M. Huibregtse, S. Gygi, and R. M. Krug.** 2005. Human ISG15 conjugation targets both IFN-induced and constitutively expressed proteins functioning in diverse cellular pathways. Proc. Natl. Acad. Sci. USA **102:**10200–10205.
57. **Zhou, A., J. Paranjape, T. L. Brown, H. Nie, S. Naik, B. Dong, A. Chang, B. Trapp, R. Fairchild, C. Colmenares, and R. H. Silverman.** 1997. Interferon action and apoptosis are defective in mice devoid of 2′,5′-oligoadenylate-dependent RNase L. EMBO J. **16:**6355–6363.
58. **Zhou, A., J. M. Paranjape, S. D. Der, B. R. Williams, and R. H. Silverman.** 1999. Interferon action in triply deficient mice reveals the existence of alternative antiviral pathways. Virology **258:**435–440.
59. **Zou, W., and D. E. Zhang.** 2006. The interferon-inducible ubiquitin-protein isopeptide ligase (E3) EFP also functions as an ISG15 E3 ligase. J. Biol. Chem. **281:**3989–3994.